Thursday, October 16, 2003
Afternoon Session I
RHEOLOGY OF MARTIAN ICE-RICH MATERIALS
1:30 p.m. Victoria Room

Greve R. * Mahajan R. A.
Influence of Ice Rheology and Dust Content on the Dynamics of the North-Polar Cap of Mars **[#8003]**

Turtle E. P. * Pathare A. V. Crown D. A. Chuang F. C. Hartmann W. K. Greenham J. C. Bueno N. F.
Modeling the Deformation of Lobate Debris Aprons on Mars by Creep of Ice-rich Permafrost **[#8091]**

Durham W. B. * Kirby S. H. Stern L. A. Circone S. C.
The Rheology of CO_2 Clathrate Hydrate and Other Candidate Ices in the Martian Polar Caps **[#8132]**

PANEL DISCUSSION
NATURE, ORIGIN, AND EVOLUTION OF
MID-LATITUDE DEPOSITIONAL MANTLES AND DEBRIS/FLOW FEATURES
Panelists: TBD

GENERAL DISCUSSION

3:30 – 3:45 p.m. BREAK

INFLUENCE OF ICE RHEOLOGY AND DUST CONTENT ON THE DYNAMICS OF THE NORTH-POLAR CAP OF MARS. Ralf Greve, *Dept. Mechanics, Darmstadt University of Technology, D-64289 Darmstadt, Germany (greve@mechanik.tu-darmstadt.de)*, Rupali A. Mahajan, *Max Planck Institute for Aeronomy, D-37191 Katlenburg-Lindau, Germany*.

Introduction. The Martian poles are both covered by ice caps. The seasonal caps, which can extend down to latitudes of approximately $55^\circ\mathrm{N/S}$, consist of only some ten centimeters of CO_2 snow which sublimes into the atmosphere during the respective summer season. The smaller residual caps poleward of approximately $80^\circ\mathrm{N/S}$ are underlain by massive topographic structures known as the polar layered deposits [11]. The complexes composed of the residual caps and the layered deposits are referred to as the north- and south-polar cap (NPC/SPC), respectively. Owing to the Mars Orbiter Laser Altimeter (MOLA) measurements of the Mars Global Surveyor (MGS) spacecraft, the surface topographies of the NPC and SPC have been mapped very precisely [10,13].

Previous studies [3,4,5] indicate that the NPC is a dynamic ice mass which shows glacial flow of the order of $1\ \mathrm{mm\ a^{-1}}$ at present. Its present topography is the result of the climatic history over the last millions of years, which was probably characterized by climate cycles as a consequence of strong, quasi-periodic variations of the orbital parameters obliquity, eccentricity and precession on time-scales of 10^5–10^6 years [7]. This idea is supported by the light-dark layered deposits of both polar caps indicating a strongly varying dust content of the ice due to varying atmospheric conditions.

In this study, the dynamic and thermodynamic evolution of the NPC will be simulated with the ice-sheet model SICOPOLIS. The boundary conditions of surface accumulation, ablation and temperature are derived directly from the solar-insolation history by applying the Mars Atmosphere-Ice Coupler MAIC developed by Greve et al. [5]. We consider steady-state scenarios under present climate conditions as well as transient scenarios over the last millions of years of climate history. A large uncertainty in model studies of that kind results from the poorly constrained rheological properties of the ice and the unknown dust content. Therefore, we will look systematically into the influence of these two aspects on the evolution of ice topography and glacial flow of the ice body. Some basic considerations for this investigation are given below.

Ice rheology. For terrestrial ice, a well-established non-linear viscous rheology which relates the strain-rate tensor $\boldsymbol{D} = \mathrm{sym\ grad}\,\boldsymbol{v}$ (velocity $\boldsymbol{v}$) to the Cauchy stress deviator $\boldsymbol{t}^{\mathrm{D}}$ is Glen's flow law,

$$\boldsymbol{D} = E A(T') \sigma^{n-1}\, \boldsymbol{t}^{\mathrm{D}}, \tag{1}$$

where $\sigma = [\mathrm{tr}\,(\boldsymbol{t}^{\mathrm{D}})^2/2]^{1/2}$ is the effective shear stress and $n = 3$ the stress exponent. The flow-rate factor depends via the Arrhenius law

$$A(T') = A_0\, e^{-Q/R(T_0+T')} \tag{2}$$

on the temperature relative to the pressure melting point, T', and for $T' \leq -10^\circ C$ suitable values for the constants are $A_0 = 3.985 \times 10^{-13}\ \mathrm{s^{-1}\,Pa^{-3}}$, $Q = 60\ \mathrm{kJ\,mol^{-1}}$ (activation energy), $R = 8.314\ \mathrm{J\,mol^{-1}\,K^{-1}}$ (universal gas constant) and $T_0 = 273.15\ \mathrm{K}$ [9]. The flow-enhancement factor E is equal to unity for pure ice and can deviate from unity due to the softening or stiffening effect of impurities in the ice. A widely used value for terrestrial ice formed during glacial periods is $E = 3$, interpreted as the softening influence of very small amounts of fine dust, approximately $1\ \mathrm{mg\ kg^{-1}}$ with particle sizes of 0.1 to $2\,\mu\mathrm{m}$ [6].

It is not clear whether the flow law (1), which describes the flow mechanism of dislocation creep, is suitable for the low temperatures and low strain rates in the Martian caps. There is strong evidence that other, grain-size-dependent flow mechanisms like grain-boundary sliding become favoured instead [1,2]. These can be described by the flow law

$$\boldsymbol{D} = E A(T') \left(\frac{d_0}{d}\right)^p \sigma^{n-1}\, \boldsymbol{t}^{\mathrm{D}} \tag{3}$$

with the stress exponent $n = 1.8$, the grain size d, the reference grain size $d_0 = 10^{-3}\ \mathrm{m}$ and the grain-size exponent $p = 1.4$. The flow-rate factor $A(T')$ is described by the Arrhenius law (2) with the parameters $A_0 = 9.826 \times 10^{-10}\ \mathrm{s^{-1}\,Pa^{-1.8}}$ and $Q = 49\ \mathrm{kJ\ mol^{-1}}$ [8].

An upper limit for the grain size d can be obtained by assuming that it is a result of normal grain growth only. From a variety of data for terrestrial polar ice masses and theoretical considerations, the growth rate

$$\frac{\mathrm{d}}{\mathrm{d}t}(d^2) = k \tag{4}$$

was derived, where t is the time and $\mathrm{d}/\mathrm{d}t$ is the material time derivative which follows the motion of the ice particles. The growth-rate parameter k depends on the absolute temperature T via the Arrhenius law

$$k(T) = k_0\, e^{-Q_k/RT}, \tag{5}$$

with the activation energy $Q_k = 42.5\ \mathrm{kJ\,mol^{-1}}$ and the constant $k_0 = 9.5\ \mathrm{m^2\,a^{-1}}$ [12]. As an example, for $T = 173\ \mathrm{K}$ this yields a growth rate of $1.40\ \mathrm{mm^2\,Ma^{-1}}$.

Dust content. Satellite imagery shows that parts of the polar caps appear dark, which indicates that they consist of ice with some amount of mixed-in dust. However, for the average volume fraction φ of dust in the ice no quantitative information is available. For modelling studies of the polar caps this is a serious problem because the dust content can affect the ice flow via direct stiffening, an increasing density and a decreasing heat conductivity which leads to basal warming. Therefore, we compute the density, ρ, and heat conductivity, κ, of the ice-dust mixture as volume-fraction-weighed averages of the

values for pure ice and crustal material,

$$\rho = (1-\varphi)\rho_{\rm i} + \varphi\rho_{\rm c}, \quad (6)$$

$$\kappa = (1-\varphi)\kappa_{\rm i} + \varphi\kappa_{\rm c}, \quad (7)$$

with the following parameters: ice density $\rho_{\rm i} = 910\,{\rm kg\,m^{-3}}$, heat conductivity of ice $\kappa_{\rm i} = 9.828\,e^{-0.0057\,T[{\rm K}]}\,{\rm W\,m^{-1}K^{-1}}$, density of crustal material $\rho_{\rm c} = 2900\ {\rm kg\,m^{-3}}$, heat conductivity of crustal material $\kappa_{\rm c} = 2.5\ {\rm W\,m^{-1}\,K^{-1}}$ [4]. Direct stiffening is described by a flow-enhancement factor $E < 1$ based on laboratory measurements of the deformation of ice-dust compounds [1],

$$E = e^{-2\varphi}. \quad (8)$$

This means that a dust content of 10% ($\varphi = 0.1$) leads to an almost 20% stiffer material compared to pure ice.

References. [1] Durham, W. B. (1998). Factors affecting the rheologic properties of Martian polar ice. *First International Conference on Mars Polar Science and Exploration*, LPI Contribution No. 953, pp. 8–9. Lunar and Planetary Institute, Houston. [2] Goldsby, D. L. and D. L. Kohlstedt (1997). Grain boundary sliding in fine-grained ice I. *Scripta Materialia 37* (9), 1399–1406. [3] Greve, R. (2000). Waxing and waning of the perennial north polar H_2O ice cap of Mars over obliquity cycles. *Icarus 144* (2), 419–431. [4] Greve, R., V. Klemann and D. Wolf (2003). Ice flow and isostasy of the north polar cap of Mars. *Planet. Space Sci. 51* (3), 193–204. [5] Greve, R., R. A. Mahajan, J. Segschneider and B. Grieger (2003). Evolution of the north-polar cap of Mars: A modelling study. *Planet. Space Sci.* Submitted. [6] Hammer, C. U., H. B. Clausen, W. Dansgaard, A. Neftel, P. Kristinsdottir and E. Johnson (1985). Continuous impurity analysis along the Dye 3 deep core. In C. C. Langway, H. Oeschger, and W. Dansgaard (Eds.), *Greenland Ice Core: Geophysics, Geochemistry and the Environment*, Geophysical Monographs No. 33, pp. 90–94. American Geophysical Union, Washington DC. [7] Laskar, J., B. Levrard and J. F. Mustard (2002). Orbital forcing of the martian polar layered deposits. *Nature 419* (6905), 375–377. [8] Nye, J. F. (2000). A flow model for the polar caps of Mars. *J. Glaciol. 46* (154), 438–444. [9] Paterson, W. S. B. (1994). *The physics of glaciers*. Third edition. Pergamon Press, Oxford etc. [10] Smith, D. E., and 18 others (1999). The global topography of Mars and implications for surface evolution. *Science 284* (5419), 1495–1503. [11] Thomas, P., S. Squyres, K. Herkenhoff, A. Howard and B. Murray (1992). Polar deposits of Mars. In H. H. Kieffer, B. M. Jakosky, C. W. Snyder, and M. S. Matthews (Eds.), *Mars*, pp. 767–795. University of Arizona Press, Tucson. [12] Thorsteinsson, T. (1996). Textures and fabrics in the GRIP ice core, in relation to climate history and ice deformation. *Reports on Polar Research 205*, 146 pp. Alfred Wegener Institute for Polar and Marine Research, Bremerhaven. [13] Zuber, M. T., and 20 others (1998). Observations of the north polar region of Mars from the Mars Orbiter Laser Altimeter. *Science 282* (5396), 2053–2060.

MODELING THE DEFORMATION OF LOBATE DEBRIS APRONS ON MARS BY CREEP OF ICE-RICH PERMAFROST. E.P. Turtle[1,2], A.V. Pathare[1], D.A. Crown[1], F.C. Chuang[1], W.K. Hartmann[1], J.C. Greenham[3] and N.F. Bueno[2], [1]Planetary Science Inst., 620 N. 6th Ave., Tucson, AZ, 85705, [2]Lunar and Planetary Lab., Univ. of Arizona, Tucson, AZ, 85721-0092 (turtle@lpl.arizona.edu), [3]California Inst. of Technology, Pasadena, CA.

Introduction: A wide variety of mid- to high-latitude surface features on Mars has long been attributed to viscous creep and flow phenomena associated with near-surface ground ice. On the basis of Viking Orbiter images, Squyres [1] identified two classes of creep-related landforms: (1) softened terrain, which results from *in situ* viscous deformation and is particularly evident in impact craters with degraded rims and flattened topographic profiles, and (2) debris aprons, which are produced by mass wasting along escarpments, *e.g.*, lobate debris aprons, lineated valley fill, and concentric crater fill. Such features have been attributed to kilometer-thick layers of permafrost (with upper boundaries less than 200 m deep) at higher latitudes [2], an interpretation that is consistent with recent *Mars Odyssey* GRS observations indicating a high water content very close to the Martian surface [3].

We are using *MGS* MOC and MOLA data to document the structural and topographic characteristics of softened landforms and debris aprons in the Hellas and Noachis regions. By comparing the observed landforms to the results of finite-element models of viscous creep relaxation, which incorporate recent laboratory measurements of ice/rock mixtures [4-6], we can constrain the conditions necessary to allow such deformation on Mars [7,8].

Observations: Debris aprons are broad, gently sloping (~1°-14°) accumulations of material at the bases of escarpments (*e.g.*, Fig. 1). They often exhibit convex-upward topographic profiles (Fig. 1B) and relatively young crater retention ages (1-100 Myr). One concentration of these features is found east of the Hellas impact basin [9]. To look for patterns between the location or nature of mountains and whether or not they exhibit debris aprons, we have characterized debris aprons in a region east of the Hellas impact basin: 30° - 40° S, 240° - 280° W. Using MOLA data we quantified a variety of attributes of mountains in the study region: latitude, longitude, maximum flank slope, total slope, total height, total width perpendicular to the long axis, and basal altitude.

Within this region the only attributes that showed even weak correlations to the existence of debris aprons were latitude and slope, and these were not statistically significant. Debris aprons are more abundant to the south of our study region, which seems consistent with the lower average annual temperatures and annual insolation if near-surface ice (the stability of which is strongly temperature dependent) plays a large role in debris apron formation. Similarly, a correlation between the existence of debris aprons and basal altitude was expected. However, despite a depletion of debris aprons in the portion of the study area within Hellas (westward of ~270°W) no correlation with altitude was observed.

We are in the process of expanding our study area down to 50° south to further investigate the effect of latitude. In this area no debris aprons are found around mountains at low elevation or west of 265° W, *i.e.*, within Hellas. We are evaluating the characteristics of mountains with and without debris aprons outside of Hellas and will combine these observations with those for mountains between 30° and 40° to look for other factors that may control ground ice distribution.

Figure 1: Example of a debris apron around a mountain near Hellas at 45ºS, 255°W. (A) MOC image (M0204416) with the approximate location of the MOLA groundtrack. (B) MOLA topographic profile (orbit 15221), vertical exaggeration ~10.

(A)

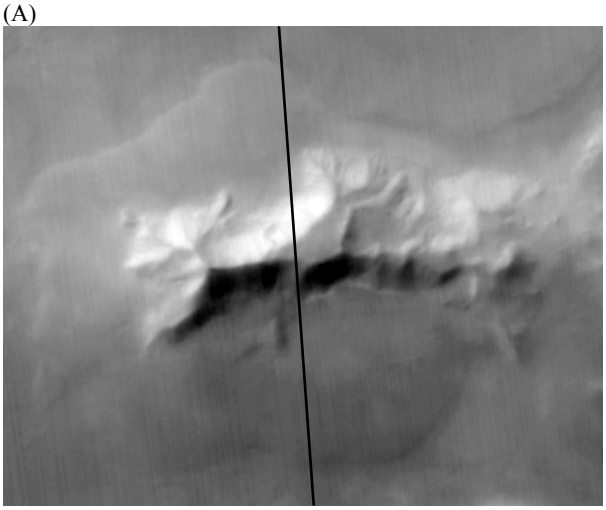

(B)

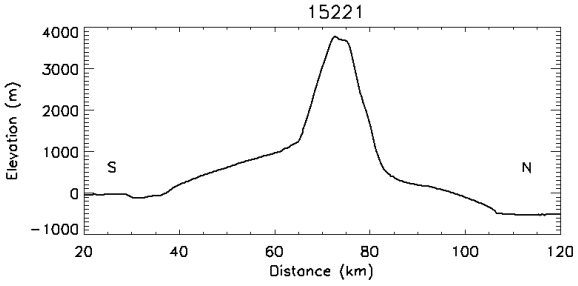

Modeling: We have applied finite-element analysis to investigate the deformation of debris aprons by creep of an ice-rich surface layer. Our models incorporate laboratory measurements of the rheological parameters for dust/water-ice mixtures undergoing dislocation creep and grain size dependent creep [4,5]; both of which are relevant under present Martian conditions: T_{surf} = 200 K [10]; dT/dz = 15 K/km [11,12]. We have built models with initial slopes ranging from 5° - 45° (*e.g.*, Figs. 2-5); slopes as shallow as ~1° have been observed for Martian debris aprons [13,9].

Fig. 2: Cross section of a finite-element model of a 45° scarp with a 1 km thick layer of 30% ice by volume (dark red), before (top) and after (bottom) 1000 yr of dislocation creep.

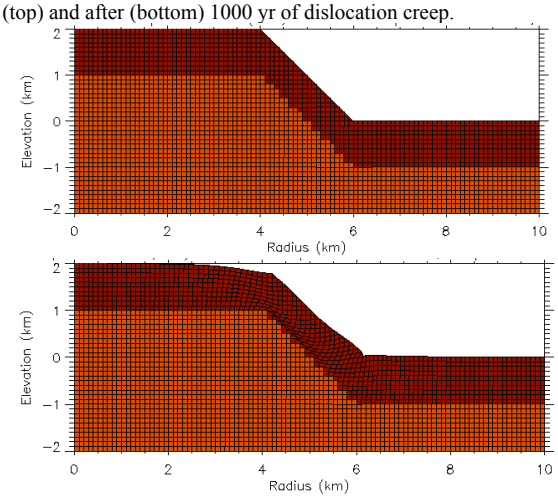

Our simulations demonstrate that the final morphology is very dependent on the initial distribution of the ice-rich material (*cf.* Figs. 3, 4) as well as on the conditions applied at the base of the ice-rich debris. Furthermore, even under present Martian conditions, viscous creep can occur quite rapidly; on timescales of 10^3-10^4 years (Fig. 5). However, if the mobility of the ice is restricted by a surface layer that resists deformation, or the high volume fractions of ice inferred to be present within a ~1 m surface layer [3] does not continue to significant depths, the deformation timescales could be significantly longer. We are also investigating the extent to which blocks of intact rock distributed within the ice-rich regolith [*e.g.*, 14] could serve to increase the deformation timescales.

Fig. 3: Cross-section of a slope of ice-rich material (uniform composition of 30% ice by volume and frictionless basal boundary) after 7500 yr of dislocation creep (basal boundary is frictionless). The solid diagonal line illustrates initial topography which is 34°, near the angle of repose.

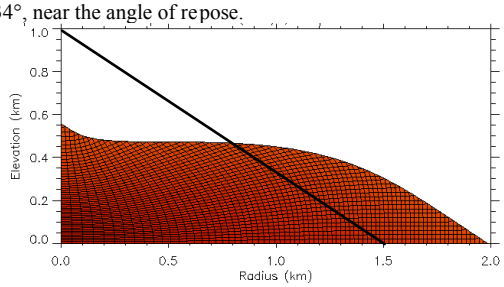

Fig. 4: Cross-section of a 500 m surface layer of ice-rich material (30% ice by volume, dark red) after 7500 yr of dislocation creep (basal boundary is frictionless). The solid diagonal line illustrates initial topography (34°).

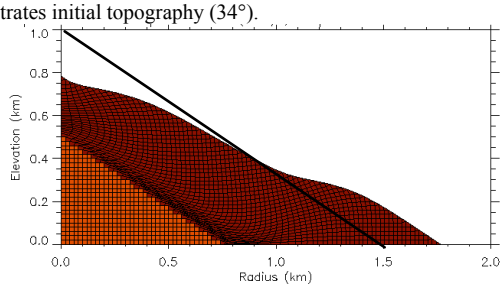

Fig. 5: This (log-log) plot of height-to-length ratio *vs.* time illustrates the rapid evolution of wedge-shaped aprons with initial slopes of 5°, 10°, and 20°. Even slopes as low as ~1° (indicated by the solid horizontal line), which are achieved in significantly less than 10^5 years, continue to deform rapidly.

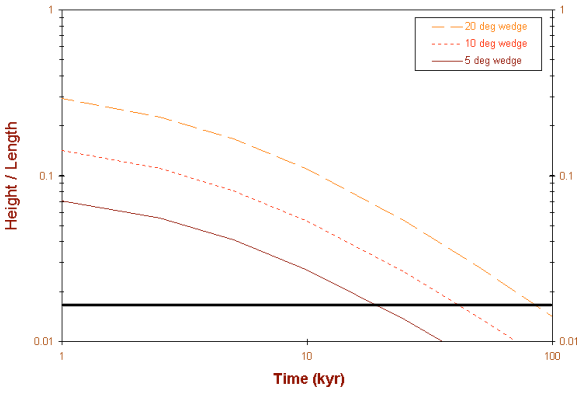

References: [1] Squyres S. (1989) *Icarus* **7**, 139-148. [2] Squyres S. *et al.* (1992) in Mars, Ed. H. Kieffer, Univ. Arizona Press, Tucson, 523-554. [3] Boynton W.V. *et al.* (2002) *Science* **297**, 81-85. [4] Durham W.B. *et al.* (1997) *JGR* **102**, 16293-16302. [5] Durham W.B. *et al.* (2000) Second Intl. Conf. on Mars Polar Sci. and Exploration, LPI Contribution #1057, 28-29. [6] Mangold N. *et al.* (2002) *Planet. Space Sci.* **50**, 385-401. [7] Turtle E.P. *et al.* (2002) *Eos. Trans. AGU, 83*, Spring Meet. Suppl., Abstract #P42A-10. [8] Turtle E.P. *et al.* (2003) *EGS/AGU* EAE03-A-07809. [9] Pierce T.L. and Crown D.A. *Icarus* **163**, 46-65. [10] Martin T.Z. (1981) *Icarus* **45**, 427-445. [11] Schubert G. *et al.* (1992) in Mars, Ed. H. Kieffer, Univ. of Arizona Press, Tucson, 147-183. [12] Clifford S.M. (1993) *JGR* **98**, 10973-11016. [13] Mangold N., Allemand P. (2001) *GRL* **28**, 407-410. [14] Whalley W.B., Azizi F. (2003) *JGR* **108**, 2002JE001864.

THE RHEOLOGY CO_2 CLATHRATE HYDRATE AND OTHER CANDIDATE ICES IN THE MARTIAN POLAR CAPS. W. B. Durham[1], S. H. Kirby[2], L. A. Stern[2], and S. C. Circone, [1]UCLLNL (P.O. Box 808, Livermore, CA 94550; durham1@llnl.gov), [2]USGS (Menlo Park, CA 94025).

Introduction: Modeling the evolution of the Martian polar ice caps requires, among other things, knowledge of the rheologies of their component phases. We review here the known flow laws for water ice and solid CO_2, which are, respectively, the major icy phase, and major CO_2-bearing phase, if conventional wisdom is to be believed. We also present first measurements on the flow of CO_2 clathrate hydrate, whose presence in the south polar cap has been suggested. Earlier measurements of methane clathrate, which is structurally analogous to CO_2 hydrate and which is dramatically harder than water ice suggested that the presence of important volumes of clathrates in the south polar cap were unlikely, owing to the exceedingly high strength of the material. The new measurements show that CO_2 hydrate is significantly weaker than CH_4 clathrate, but still much stronger than water ice. Thus, the rheological basis for dismissing CO_2 hydrate is somewhat weakened, but relaxation models for the south polar cap are still inconsistent with the strength of CO_2 clathrate. Concerning the water ice phase in the polar caps, it is important to consider the balance between grain-size-sensitive (GSS) and grain-size independent (GSI) mechanisms of creep.

Background: Laboratory experimentation on ices is aimed at providing a constitutive rheological law, typically of the form

$$\dot{\varepsilon} = A\sigma^n \exp(-Q/RT) \qquad (1)$$

where $\dot{\varepsilon}$ is the ductile (permanent, volume conservative) strain rate, σ is differential stress, T is temperature, R is the gas constant, and the three parameters A, n, and Q are material-specific constants. It is possible to duplicate Martian temperatures and Martian differential stresses in the laboratory, but it is not possible to duplicate them simultaneously because the resulting Martian strain rates will be too low to measure on the laboratory time scale. While we endeavor to reach ever finer levels of resolution, the current limit on laboratory strain rates, about 2×10^{-8} s^{-1}, is still several orders of magnitude faster than strain rates in the spreading Martian polar caps.

Experimental measurements: The pure phase rheological properties have now been measured in the laboratory for most of the candidate Mars polar cap materials [1-4], and in the case of water ice, a distinction has also been discerned between a GSS and GSI rheology. Conveniently, there are some rather extreme rheological contrasts between some of the phases. In particular, the effective viscosity (proportional to $\sigma/\dot{\varepsilon}$ in Eq. 1) of pure CO_2 ice is several orders of magnitude lower than that of water ice, and the strength of gas hydrates is several orders of magnitude higher than that of water ice. The Mars polar caps are therefore unlikely to hold large reservoirs of CO_2 either as solid CO_2, because the caps would have relaxed far below their current profiles, or as hydrate, because they would not have flowed at all, contrary to what observational evidence suggests.

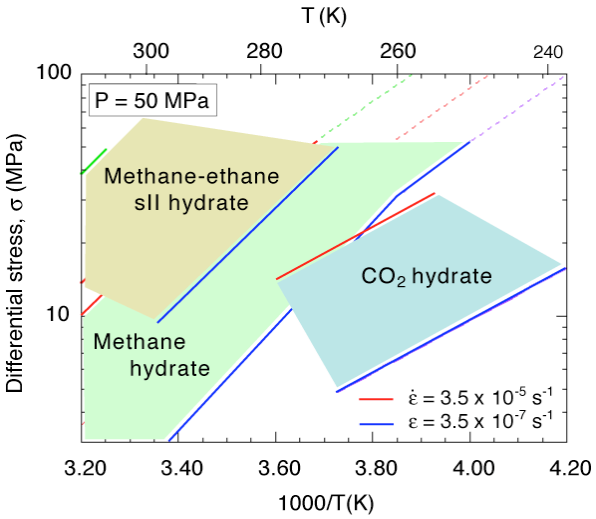

Figure 1. Laboratory measured rheologies of three different gas clathrate hydrates. Methane and CO_2 clathrate are both so-called structure I clathrates, while the methane-ethane clathrate as tested is a structure II material. Fields are bounded by lines of constant $\dot{\varepsilon}$, following Eq. (1)

The latter conclusion was based on the measured strength of methane clathrate, a common earth material with a structure identical to that of CO_2 clathrate. We have now measured the flow of CO_2 clathrate itself (Fig. 1), and found it to be considerably weaker—by about two orders of magnitude in viscosity—than methane clathrate. Although the CO_2 clathrate is still two orders of magnitude more viscous than water ice at similar conditions, the conclusion is now less robust, at least on rheological grounds, that important volumes of CO_2 clathrate cannot exist in the Mars polar caps. We

may have to wait until Mars geology is better understood before we can make additional conclusions.

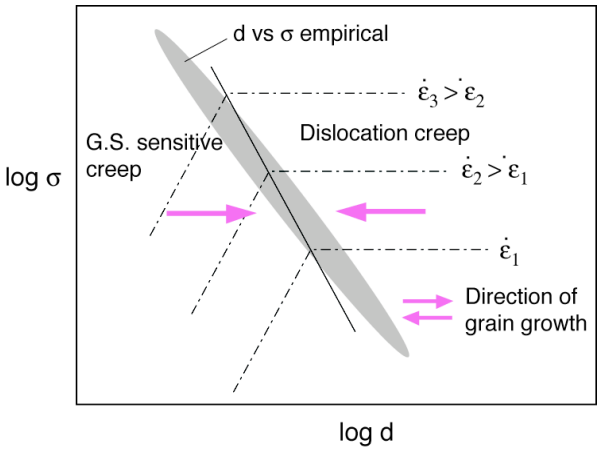

Figure 2. Theoretical evolution of grain size during GSS and GSI (here: dislocation creep) creep, and its effect on steady-state. Grain size tends to increase during GSS creep, but decrease during GSI creep, thus working at cross purposes with respect to the host mechanism. (from [5]).

There is one point we wish to emphasize regarding the rheology of polycrystalline water ice, which is likely to be the major phase in the Mars polar caps. Goldsby and Kohlstedt [1] were able to activate and quantify a GSS rheology in ice, one of the few materials where this has been possible in the laboratory. The finding is quite important to geology and planetary geology because GSS mechanisms are ordinarily less stress sensitive than GSI mechanisms ($n \approx 2$ vs $n \approx 4$ in Eq. 1) and therefore would tend to be favored over GSI mechanisms at the very low stresses and strain rates typical of geological settings.

However, caution should be applied when modeling glacier flow with GSS creep. As pointed out by de Bresser and colleagues [5], one finds many instances in natural settings on Earth (in calcite- and olivine-bearing rocks in particular) where the observed grain size and inferred strain rate imply conditions, following Eq. (1), such that the strain rates contributed by GSS and GSI creep are roughly comparable. Figure 2 offers an explanation for such a phenomenon. Since GSI creep usually involves the movement and growth of dislocations, internal energy of individual grains tends to increase with strain. Since internal energy tends to drive recrystallization, which in turn often results in finer grain sizes, grain size can decrease during GSS creep (the left-pointing red arrow in Fig. 2). GSS creep depends on the presence of grain boundaries in the material, so this action of GSI creep to decrease grain size can have the effect of increasing the proportion of strain rate contributed by GSS creep. On the other hand, deformation by GSI creep takes place by the rigid slip of grain boundaries or by the transport of material along grain boundaries, neither of which changes the internal defect structure or therefore the internal energy of grains. The grains may therefore grow under the motivation of ordinary surface energies (right-pointing arrow in Fig. 2).

The combined result of GSS and GSI creep working at cross purposes with respect to grain growth is that we might expect a balance to eventually be struck, with both mechanisms contributing to flow. In modeling the flow of ice in the Martian polar caps, both flow laws (Eq. 1) for GSS and GSI should be considered.

References: [1] Goldsby D.L. and Kohlstedt, D.L. (1997) *Scripta Mater.*, *37*, 1399-1406. [2] Durham W. B., Stern L. A., and Kirby S. H (1999) *Geophys. Res. Lett.*, *26*, 3493-3496. [3] Durham W. B. and Stern L. A. (2001) *Annu. Rev. Earth Planet. Sci.*, *29*, 295-330. [4] Durham W. B., Kirby S. H., Stern L. A., and Zhang W. (2003) *JGR*, *108*(B4), 2182, doi:10.1029/2002JB001872. [5] de Bresser J. H. P., ter Heege J. H., Spiers C. J. (2001). Grain size reduction by dynamic recrystallization: Can it result in major rheological weakening? *Int. J. Earth Sci., 90,* 28. doi 10.1007/s005310000149